Common Product Neurons

Luciano da Fontoura Costa
luciano@ifsc.usp.br

São Carlos Institute of Physics – DFCM/USP

1st Nov. 2021

Abstract

The present work addresses a comparative performance of artificial neurons obtained in terms of the recently introduced real-valued Jaccard and coincidence indices and respective functionals. The interiority index and classic cross-correlation are also included in our study. After presenting the basic concepts related to multisets and the adopted similarity metrics, including new results about the generalization of the family of real-valued Jaccard and conicidence indices to higher orders, we proceed to studying the response of a single neuron, not taking intoaccount the output non-linearity (e.g. sigmoid), respectively to the detection of a gaussian stimulus in presence of displacement, magnification, intensity variation, noise and interference from additional patterns. It is shown that the real-valued Jaccard and coincidence approaches are substantially more robust than the interiority index and the classic cross-correlation. The coincidence based neurons are shown to have the best overall performance for the considered type of data and perturbations. The reported concepts, methods, and results, have substantial implications not only for patter recognition and deep learning, but also regarding neurobiology and neuroscience.

"Flower patches on the hill, never the same along the years.'

LdaFC

1   Introduction

A great deal of human perception and cognition, as well as of many other living beings, relies on the neuronal transduction and processing of several types of information. From a simplified mathematical perspective, a neuron has been understood to involve two main stages: (i) an inner product between the input stimulus and the respective synaptic weights, yielding an accumulated value; and (ii) the application of a non-linear function, such as a sigmoid, over that value, yielding or not an action potential (e.g. [1, 2]).

This type of operation can be effectively summarized in the concept of *receptive field* (e.g. [3]) respectively defined in some input stage space. For instance, the ganglion cells of the retina have been characterized by respective receptive fields defined in the visual space (scene) or along the retina surface. The mathematical modeling of these receptive fields therefor provides an effective manner for representing and better understanding neuronal operation according to a systemic representation which is directly related to the concepts of correlation, convolution and point-spread functions.

In addition to its dynamic properties along time, the shape of receptive fields has been understood to play an important role in detecting and processing information. Indeed, a more elaborated dendritic arborization will tend to have enhanced chances of receiving synaptic connections. The importance of the neuronal geometry seems to be so important that it often adapts to the type of function the neuron performs.

In the present work, we re-assess the functioning of single neurons in terms of recently introduced multiset-based similarity indices. More specifically, instead of using the traditional inner product, we apply the real-valued Jaccard, interiority, and coincidence similarity metrics [4, 5, 6]. Of particular interest is the fact that, though extremely simple, these metrics implement an action that, though analogous to the classic inner product, is non-linear as a consequence of the use of the maximum and minimum binary operators (in the sense of having two arguments).

We start by presenting the basic multiset concepts (e.g. [7, 8, 9, 10, 11, 12]), as well as the recently introduced real-valued Jaccard and coincidence indices [4, 5, 6]. In addition to discussing the intrinsic, though limited, ability of the real product between two scalars in providing information about their respective similarity, we shown how the common product and real-valued Jaccard index

can be derived in a logical manner starting from the totally strict similarity comparison provided by the Kronecker delta function. Unlike in a recent study [4], which approached the subject of similarity more generally, the neuronal perspective adopted in this work allowed attention to be focused on similarity comparisons where one of the arguments are kept constant, therefore corresponding to stable synaptic weights. New results are reported regarding the generalization of the multiset similarity indices to higher orders, yielding a generic similarity function that converges to the Kronecker delta product for infinite order.

A systematic approach is then proposed and applied for comparing the performance of neurons in pattern recognition, while adopting the standard cross-correlation as well as the interiority, real-valued Jaccard and coincidence indices [4, 5, 6]. The comparison is performed with respect to varying patter position, intensity, scale, noise levels, and presence of additional interfering patterns.

Several interesting results are obtained that, overall, confirm that the coincidence index provides the most strict and detailed recognition, followed by the real-valued Jaccard and interiority indices. The classic cross-correlation resulted almost useless for the considered task and type of data. These results have many implications and applications to several related areas, some of which are also briefly discussed.

2 The Common Product and Related Indices

Given any two real values x and y, their product constitutes one of the most frequently performed algebraic operation in science and technology, not to mention daily activities.

There are some quite interesting properties of the product xy that, perhaps as a consequence of being so ubiquitous, are not commonly realized. The first is that the product follows the following sign rule:

$$
\begin{array}{cc|c}
sign\,\{x\} & sign\,\{y\} & sign\,\{xy\} \\
\hline
- & - & + \\
- & + & - \\
+ & - & - \\
+ & + & + \\
\end{array}
\tag{1}
$$

Consequently, the classic product between two real values is capable of expressing whether the two values x and y point toward the same direction along the real line, in which case $sign\,\{xy\} = +1$, or if they oppose one another, yielding $sign\,\{xy\} = -1$.

This important property of the classic real product hints at a yet more important respective feature, namely the fact that *the classic real product provides a measurement of similarity* between the two values x and y [4]. It is this particular feature of the product that confers to the inner product between two vectors some ability for quantifying the similarity of those vectors. More specifically, the traditional inner product between any two vectors $\vec{v}$ and $\vec{p}$ in an $N-$dimensional space is defined as:

$$
\langle \vec{v}, \vec{p} \rangle = \sum_{i=1}^{N} v_i p_i = |\vec{v}|\,|\vec{p}|\cos(\theta)
\tag{2}
$$

where θ is the smallest angle between the two vectors. Provided the magnitudes of $\vec{v}$ adn $\vec{p}$ are kept constant, the inner product will provide an indication of the angular and orientation similarity between these two vectors.

However, the potential of the scalar product as a similarity property is hard to be realized because it varies so much with the magnitude of x and y. Nevertheless, provided we have that $|x| \leq 1$ and $|y| \leq 1$, we have that $-1 \leq xy \leq 1$.

Despite its intrinsic ability for quantifying similarity, as well as it extensive application in operations as the inner product, the real product has two important shortcomings. First, it is relatively difficult to be implemented in computational hardware or even in analog circuits. Second, it has been shown that the real product tends to be too tolerant regarding the provided indication of similarity [6, 4].

Similarity measurements are typically performed by binary operators, which is the mathematical term for indicating that the operation takes two values as input.

The considered neuronal operation as a quantification of similarity addressed in this work provides an interesting perspective from which to address this operation. More specifically, if we consider that the similarity is to be measured between the synaptic weight y and respective input x, we can simplify the otherwise binary operation as an operation only on x, with y being understood as a parameter. Figure 1 illustrates the real product seen from this perspective, assuming synaptic weight $y = 2$.

This result well-illustrates the limitation of the traditional real product for quantifying similarity. Though the similarity will increase for $|x|$ increasing from 0 to 1, it will continue to increase thereafter. In fact, we have that:

$$
\lim_{x \leftarrow \infty} = \infty
\tag{3}
$$

As developed in [4], the prototypical function for quantifying similarity in the most strict manner possible consists in the Kronecker delta function, which can be written as:

$$
\delta_{x,y} = \begin{cases} 1 & whenever\ x = y \\ 0 & otherwise \end{cases}
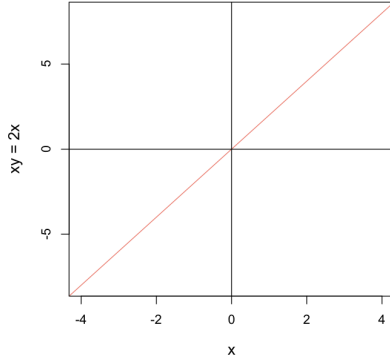\tag{4}
$$

Figure 1: The quantification of similarity between two real values as implemented by the real product xy, with $y = 2$. Effectively, this curve would indicate how similar to 2 the values of x are.

Though this function cannot provide information about the alignment of the values x and y, it can be readily modified as:

$$\tilde{\delta}_{x,y} = \begin{cases} 1 & whenever\ x = y \\ -1 & whenever\ x = -y \\ 0 & whenever\ |x| \neq |y| \end{cases} \quad (5)$$

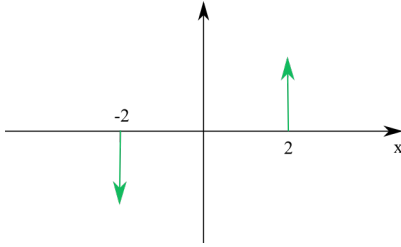Figure 2 illustrates this function for $y = 2$, i.e. $\tilde{\delta}_{x,2}$.

Figure 2: The Kronecker function modified to take into account the relative alignment of the real values x and $y = 2$, which is now reflected in the respective sign.

The problem with this generalized Kronecker delta function is that it is simply too strict in its evaluation of the similarity between x and y.

Remarkably, there is another particularly interesting possibility to quantify the similarity between two real values, and it involves the so-called *common product* [6, 4]:

$$x \circ y = s_{xy} \min \{s_x x, s_y y\} \quad (6)$$

where $s_x = sign(x)$, $s_y = sign(y)$, and s_{xy} is the *conjoint sign function* $s_{xy} = s_x s_y$.

This function was developed [4, 5, 6] by applying multiset concepts (e.g. [7, 8, 9, 10, 11, 12]). In particular, it can be understood as a modification of the intersection between two functions in order to consider the common or

shared area of the functions with respect to the horizontal axis, hence the name *common*.

Observe that the term *common product* has been used [6, 5, 4] also to identify the functional over the elementwise application of the above equation. For simplicity's sake, we will use this terminology in a common manner, as the respective context should be enough for specifying if it is being meant its application elemenwise or as a functional.

Interestingly, this product has surprising properties, including: (i) it is extremely simple to be implemented, e.g. in electronic circuits [13]; (ii) it is conceptually simple; (iii) it obeys the sign rules in Equation 1; and (iv) it implements a much more strict quantification of similarity than the conventional product [4] which is, at the same time, more tolerant and than the generalized Kronecker delta function above.

It is therefore interesting to consider this function from the neuronal perspective, i.e. with one of its values kept constant. Figure 3 illustrates the common product for $y = 2$.
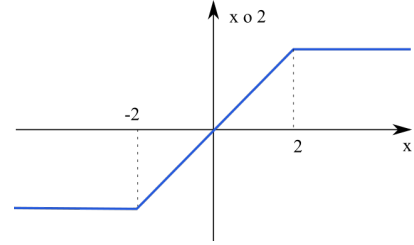

Figure 3: The common product assuming $y = 2$, i.e. $x \circ 2$. Now we have that $-2 \leq x \circ 2 \leq 2$.

It is now clear that the common product with one of its argument kept constant corresponds to a clipped version of the real product $2x$. The saturation of the common product for $x > 2$ is a critical feature in which it implies $x \circ y$ to become bound by the fixed value.

However, maximum similarity will be observed for any value of x larger than 2. An interesting manner to circumvent this problem consists of normalizing the common product as follows:

$$J_R(x, y) = \frac{s_{xy} \min \{s_x x, s_y y\}}{\max \{s_x x, s_y y\}} \quad (7)$$

so that $-1 \leq x \circ y \leq 1$. This normalized version of the common product corresponds to the *real-valued Jaccard index* applied to two scalar values [4, 5, 6].

Figure 4 illustrates both the function $n(x, y) = \max \{s_x x, s_y y\}$ and the resulting real-valued Jaccard index.

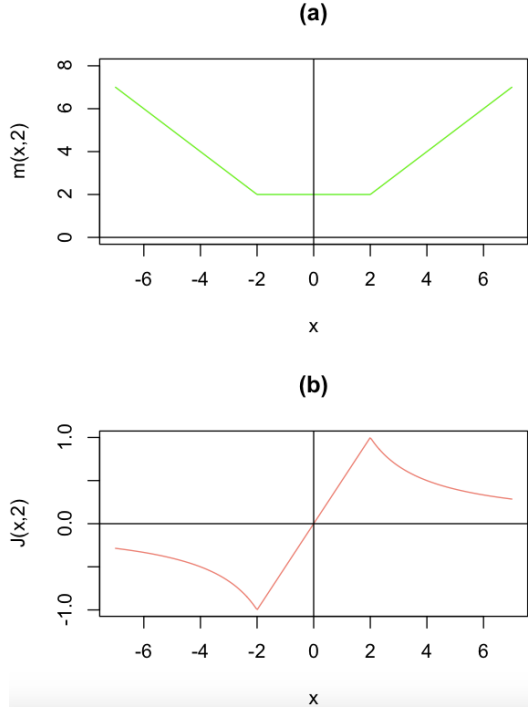The normalizing function has a direct correspon-

3

(a)

(b)

Figure 4: The normalizing function $n(x,2) = \max\{s_x x, 2\}$ and the normalized common product, which becomes the real-valued Jaccard index $J(x,2)$ applied to scalar values.
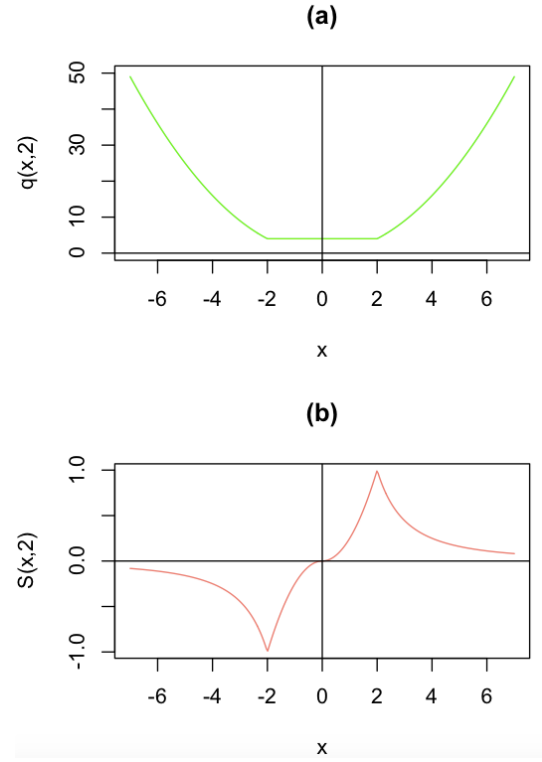
(a)

(b)

Figure 5: The normalizing function $n(x,2) = \max\{s_x x, 2\}$ and the normalized common product, which becomes the real-valued Jaccard index $J(x,2)$ applied to scalar values.
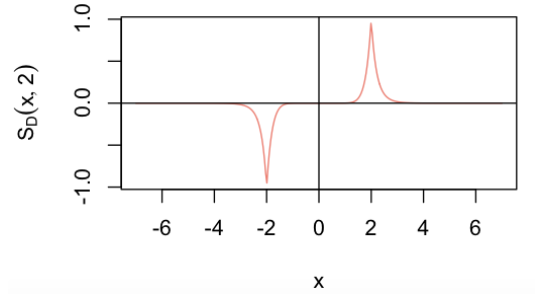

Figure 6: Even sharper similarity quantification through the function $S_{D=10}(x,2)$.

dence with the multiset concept of real-valued functions union [5]. Observe that this function increases linearly with x. As a consequence, the division of the common product by the normalizing function will penalize the similarities fro $|x| > 2$, yielding to two respective peaks in the real-valued Jaccard index $J(x,2)$. Interestingly, this resulting index can therefore be understood as a more tolerant version of the generalized Kronecker delta (compare Figs. 2 and 4b).

The developments presente above make it clear that it is possible to define an infinity of other similarity indices. For instance, it is possible to control the sharpness of the similarity peaks by using other products and normalizing functions. As an example if even sharper peaks are required, we can make:

$$S_2(x,y) = \frac{s_{xy}\left[\min\{s_x x, s_y y\}\right]^2}{\sqrt{\max\{x^2, y^2\}}} \tag{8}$$

Figure 5 illustrates this function for $y = 2$.

The above development can be generalized to any degree D even as:

$$S_D(x,y) = \frac{s_{xy}\left[\min\{s_x x, s_y y\}\right]^D}{\sqrt{\max\{x^D, y^D\}}} \tag{9}$$

Observe that the similarity function $S_D(x,y)$ tends to

the generalized Kronecker delta function when $D \leftarrow \infty$, i.e.:

$$\lim_{D \to \infty} S_D(x,y) = \tilde{\delta}(x,y) \tag{10}$$

However, for simpilcity's sake, we will consider only the real-valued Jaccard index in our subsequent performance analysis, which can be understood as the above construction when $D = 0$. A more systematic study of higher values of D will be reported elsewhere.

Now, the functional version of the common product can be stated [4, 5, 6] as:

$$\ll f(x), g(x) \gg = \int_S s_{fg}\min\{s_f f, s_g g\}\, dx \tag{11}$$

4

where $f(x)$ and $g(x)$ are real functions and S is their common support.

We can immediately make:

$$J_R(x,y) = \frac{\int_S s_{fg} \min\{s_f f, s_g g\} \, dx}{\int_S \max\{s_f f, s_g g\} \, dx} \quad (12)$$

Observe that the functional versions of the real-valued Jaccard index performs a division of functionals instead of a functional of a division. This is an important consequence of of both $f(x)$ and $g(x)$ being considered to correspond to generalized versions of multisets to real values [4, 6, 5].

The fact that traditional Jaccard index has been shown [6] not to be able to take into account the relative interiority between the two compared sets motivated the *coincidence index*, which combines the real-valued Jaccard index with the interiority (or homogeneity) between the two functions.

The interiority index for real valued functions can be expressed [4, 6, 5] as:

$$I(x,y) = \frac{\int_S \min\{s_f f, s_g g\} \, dx}{\max\{S_f, S_g\}} \quad (13)$$

where $S_f = \int_S s_f f(x) dx$ and $S_g = \int_S s_g g(x) dx$.

So that the *coincidence index* expressing the similarity between the two functions $f(x)$ and $g(x)$ can be simply expressed as:

$$c(x,y) = J_R(x,y)I(x,y) \quad (14)$$

Observe that the type of denominator in the interiority Equation 13 avoids a respective scalar version as developed above for the real-valued Jaccard index. For the same reason, it is also not viable to derive a scalar version of the coincidence index. At the same time, higher order versions of the coincidence index can be readily obtained in a manner analogue to the above developments.

Discrete respective versions of the above equations are adopted in the following developments.

3 Single Neuron Comparison

In this section, we perform a comparison of single neurons defined respectively to the real-valued Jaccard, interiority, and coincidence indices, as well as to the classic inner product.

This comparison is developed by taking into account several possible effects commonly found regarding pattern recognition by single neuronal cells, including: (a) relative position displacements; (b) stimulus size variation; (c) stimulus intensity variation; (d) noise; and (e) presence of more than a single pattern in the stimulus.

The reference input stimulus will be a circularly symmetry two-dimensional gaussian function centered at the stimulus space, given as:

$$g(x,y) = e^{-0.5\left(\frac{d(x,y)}{\sigma}\right)^2} \quad (15)$$

$$where: d(x,y) = \sqrt{x^2 + y^2} \quad (16)$$

Unless stated otherwise, we adopt $\sigma = 100$ in an 200×200 image support.

Figure 7 presents the values of the four considered methods respective to relative displacements from 0 to 30 discrete steps (pixels). Full similarity has been duly identified by all methods regarding null displacement, as could be expected. However, as soon as one of the patterns shifts, the values of all indices are decreased. The sharpest decrease is verified for the coincidence approach, which is known [6, 4] to provide a more strict quantification of pairwise similarity. The classic cross correlation presented the slowest decrease between all methods, except for displacements above 12 pixes, in which case all the indices values are already very small. This is in agreement with the identification of product based similarities [6, 4] to be particularly tolerant to pairwise differences. The real-valued Jaccard approach yielded the second fastest decreasing values.
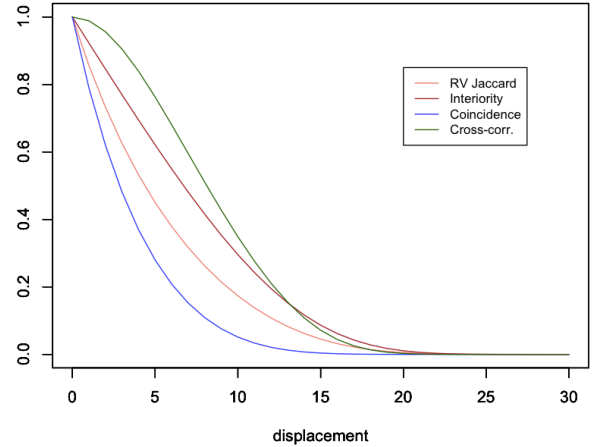

Figure 7: Similarity values obtained by the four considered methods respectively to relative displacements of two identical gaussians. The coincidence method allowed the fastest, and therefor most strict, quantification of the similarity, while the classic cross correlation yielded the most tolerant and least discriminative results.

Next, we analyse the similarity quantification in terms of varying intensities of one of the two identical gaussians, though one of them was displaced by 2 pixels along both axes in order to impose a more challenging similarity quantification. The considered intensity changes varied in a range from 0 to 3. The results are depicted in Figure 8.
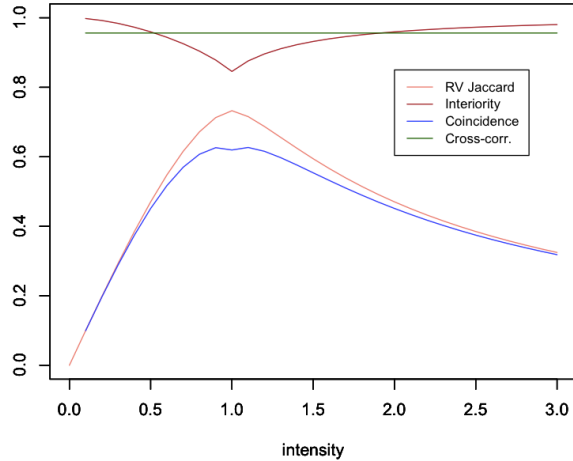
Figure 8: Quantification of the similarity between two circularly symmetric gaussians with the same dispersion, but one of them multiplied by a scaling factor from 0 to 3. In order to impose a more challenging demand, one of the gaussians was always shifted by 2 pixels along each axes. The best results are again observed for the coincidence method, followed by the real-valued Jaccard and interiority approaches. The classic cross correlated revealed to be completely insensitive to the intensity changes.
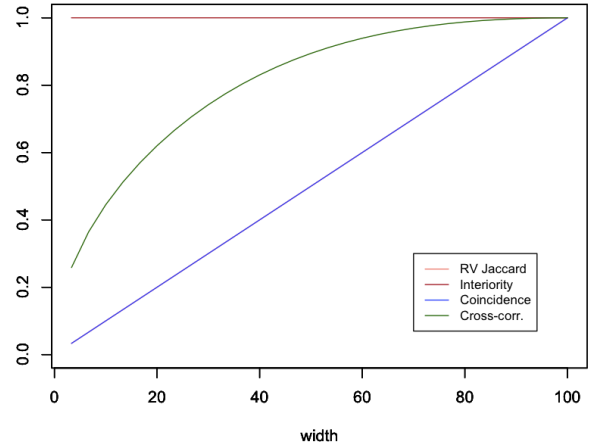

Figure 9: The similarity between the two patterns in terms of the variation of the width, corresponding to the standard deviation, of one of them. The similarity for the real-time Jaccard and coincidence approaches varies linearly from 0 to 1. The cross correlation presents a steep initial variation followed by a saturation. The kept constant at 1, which is expected given that one of the patterns is always interior to the other.

Particularly interesting results can be discerned from this figure. Of greatest notice is the complete insensitivity of the classic cross-correlation method to the intensity variations. Though this feature can be helpful in some applications where intensity variance is desired, it will completely fail in cases where more strict quantifications of similarity are required to take into account also the relative intensities. The best results in this sense have been obtained with respect to the coincidence methodology, followed by the real-valued Jaccard, and then the interiority.

It is also worth noticing that the two multiset-based methodologies present two main behaviors. From intensities ranging from 0 to 1, meaning that one of the patterns is less intense than the reference, both these methods present an almost linear increase up to identical intensity. The maximum similarity value 1 was not obtained in this case because of the small imposed relative displacement of 2 pixels along each axes. From this peak, the similarity values then decrease progressively as the intensities, which now correspond to magnifications, increase.

The results of the study of the effect of the pattern width on the respective matching is shown in Figure 9. The width, which corresponded to the standard deviation of the circularly symmetric gaussian, given in Equation 15, varied from 0 to 100.

Both the real-valued Jaccard and the coincidence match values presented a linear increase from 0 to 1. The clas-

sic cross-correlation presented an initially steep increasing profile followed by a saturation. As expected, the interiority index was kept constant with value 1, reflecting the fact that one of the patterns is always interior to the other in this particular experiment. The real-valued Jaccard and coincidence indices represent a suitable choice in case the similarity is to reflect the width discrepancy in a linear manner. The classic cross correlation again resulted more tolerant to the implemented variation, reaching relatively high values sooner than the multiset-based methods.

We now proceed to the consideration of additive symmetric uniform noise to one of the patterns. More specifically, the following noise levels are added:

$$X[x, y] = X[x, y] + \frac{i}{N_{ns}}[u(x, y) - 0.5] \qquad (17)$$

with $i = 0, 1, \ldots, N_{ns}$ and where $u(x, y)$ is a scalar uniform random field taking values in $[0.1]$. We henceforth adopt $N_{ns} = 20$. A total of 20 experiments were performed for each of these levels, the respective average and standard deviation being then considered as results.

Figure 10 illustrates the similarity values obtained by the four methods with respect to increasing levels of noise. Several aspects of interest can be identified from this figure. First, we have that the interiority similarity accounts for the slowest decreasing similarity values. This can be explained by the fact that the noisy versions of one of the patterns, despite being jagged, will be mostly interior to the other. The fastest decreasing profiles are those obtained for the real-valued Jaccard and coincidence methods, which also resulted very similar one another. This indicates that these two multiset-based approaches are

the most sensitive to the pattern modifications induced by the increasing levels of noise. The classic cross-correlation yielded an intermediate result between the interiority and multiset-based methods, again reflecting its increase tolerance to perturbations.
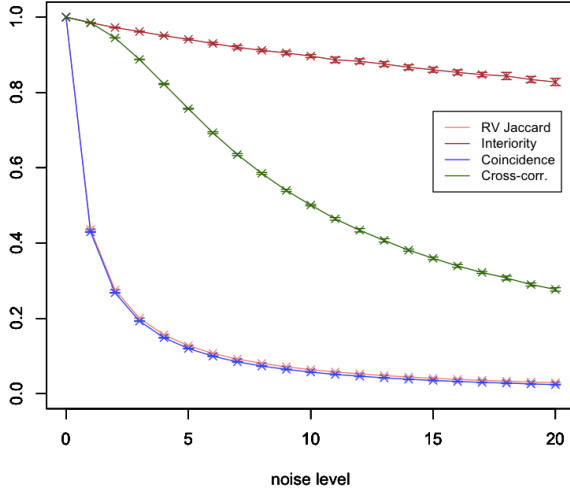

Figure 10: Similarity values obtained by the four considered methods respectively to increasing noise levels. The interiority approach is the most tolerant, followed by the classic cross-correlation, and then the two multiset-based methods. Though these curves correspond to respective averages ± standard deviations, the latter are generally very small to be visualized.

The last considered type of perturbation concerns the signed addition of whole gaussian patterns into one of the images. From 1 to 5 such patterns have been added into one of the images at uniformly random positions. The results are shown in Figure 11.

While the interiority and classic cross-correlation presented total tolerance to the added interference, a moderate discrimination can be observed in the case of the real-valued Jaccard and coincidence results, which present total overlap in the figure.

All in all, the several analysis reported in this section further substantiated the tendency of the multiset-based approaches to provide a more accurate and discriminative quantification of the stimulus recognition than the interiority and cross-correlation based methods. Significant differences in the specificity of the response have been observed in several cases, especially varying intensities, widths, and noise. Given their markedly more strict and discriminative characteristics, the real-valued and Jaccard, and even more so the coincidence approach, therefore correspond to the best choice, among the considered possibilities, for implementing pattern recognition with high levels of accuracy.
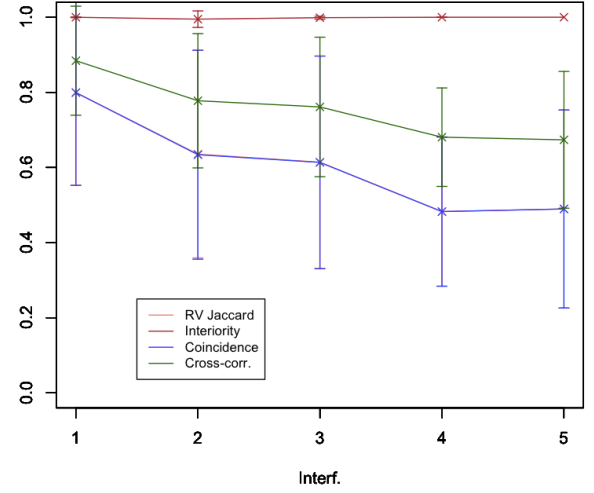

Figure 11: Similarity values obtained in presence of added interference corresponding to signed addition of from 1 to 5 gaussian patterns at uniformly random positions in the image. The curves correspond to the average ± standard deviations. Identical results have been obtained for the real-valued Jaccard and coincidence based similarities.

There is an important issue to be further discussed here, and it regards the interplay between discriminative and tolerant (or invariant) performance. One first important point concerns the fact that these are opposite properties, in the sense that a neuron that is too tolerant will provide no specific response, and vice versa. Another critical issue concerns the fact that, taken independently, neither of these two properties are necessarily good or bad. As in an engineering problem, the best solution will be that which best suits the specific requirements.

However, in the context of effective recognition of several types of patterns in the real world, in presence of all the considered perturbations, perhaps the proper solution is a balanced combination of discriminative and tolerant abilities. Actually, there is a formal solution to this duality between specificity and generality that is not so often realized. It concerns the fact that it is indeed possible to achieve both characteristics in a synergistic manner, not as a kind of trade-off or balance. This solution consists in having sets of neurons, each of which highly discriminative and specific, whose combined operation provides for the requested levels of tolerance and generalizations.

Thus, while each instance of the presented pattern will be accurate and specifically identified accurately by successive individual cells. However, at the overall group level, substantial tolerance will be achieved for several instances and perturbations of the presented stimuli. Nevertheless, this ideal architecture can only be achieved at expense of substantial informational resources, be then biological or artificial. These flexible *and* highly discrim-

inative ensembles, which constitute the ideal solution for many circumstances, are henceforth denominated *synergistic neuronal systems.*

The immediate consequence of the above considerations is that it becomes critically to have the means for implementing strict, discriminative pattern recognition at the smallest informational and energetic expenses. From this perspective, the multised-based similarity identification constitute a particularly interesting resource given their conceptual and informationally simple operation, allied to their substantially more strict and discriminative operation as verified in this work with respect to several perturbations and in [14] with respect to coexisting patterns.

Interestingly, it has been proposed recently that the multiset-operations can be implemented in extremely efficient manner in analog electronics, using only a few operational amplifiers and analog switches [13], which makes the mutiset-based approaches, and in particular the coincidence index, components of choice for the development of real-time pattern recognition systems.

It remains an issue of great interest to contemplate how befitted for implementation in biological hardware the multiset-operations ultimately are.

4   Concluding Remarks

The present work has developed a study of the application of the multiset-derived similarity indices, especially the common product, to artificial and biological neurons. More specifically, these indices are considered for substituting the inner product performed between the image stimulus and respective matrix of synaptic weights.

After presenting an overview of the related multiset concepts and developments that led to the real-valued Jaccard and coincidence index, including new results regarding higher order respective versions, we proceeded to a systematic comparison of artificial neurons performing pattern recognition in presence of several types of perturbations. More specifically, the pattern to be recognized is stored in the synaptic weights, while the similarity comparison is performed by using the several considered indices.

The results largely confirm the enhanced potential of the coincidence index, followed by the real-valued Jaccard index, for performing strict similarity quantification. This makes these types of artificial neurons primary choices for implementations and applications involving strict patter recognition. The duality between specificity and generality in this type of task has also been discussed, and it has been argued that the ideal solution is to have large ensembles of highly specific and strict neurons, each of

which adapted for taking into account specific geometric transformations so as to allow respective invariance.

Now, a particularly interesting issue arises regarding the fact that, given the substantial advantages of neurons based on the coincidence or real-valued Jaccard indices, why would they have not been adopted in biological neuronal networks aimed at effective pattern recognition? Why would the otherwise much less efficient inner product be instead implemented by the dendritic integration of the synaptic input?

There are two possible answers to this important question. First, we have that the biological hardware is intrinsically unsuitable for implementing the multiset-related operations. Interestingly, recent developments have shown that these operations can be very effectively implemented in analog hardware [13], but this does not necessarily extend to biology, though much of the neuronal operation is a correlate of electric and even electronic counterparts. If that is so that biology is intrinsically unsuitable for performing multiset-operations, these alternatives remain valid for implementations in other types of hardware.

The second possible answer is that the biological neuronal cells actually implement multiset-related functions. Indeed, consider the profile of the common product shown in Figure 3, which is the basis for all effective indices developed and applied in the present work. This function, which resembles a sigmoid, could be applied not at the implantation cone, but at each of the synapses. Indeed, the observed saturation could correspond to the saturation of the synaptic activation and/or of the local polarization of the interior of the cell. The sum corresponding to the numerator of Equation 7 would then correspond to the combination of the diffusive charge effect at the implantation cone. As for the denominator of that same equation, it is possible that other intracellular mechanisms are activated by the synaptic activity that effectively contribute to the inhibition of the action potential. These inhibitory effects could be similarity integrated at the implantation cone, accounting for the denominator in Equation 7. Though these are currently hypothetical, further consideration and experimental developments can help verifying these possibilities.

The concepts, methods, and results reported in the present work have several potential implications in a wide range of areas, including neuroscience and pattern recognition, therefore paving the way to a large number of further developments. Some examples include further studies of the possible relationships with biological cells, the consideration of other types of stimuli, as well as the evaluation of the here introduced higher order versions of the real-valued Jaccard and coincidence indices.

References

[1] S. Haykin. *Neural Networks And Learning Machines.* McGraw-Hill Education, 9th edition, 2013.

[2] L. da F. Costa. *Shape Classification and Analysis: Theory and Practice.* CRC Press, Boca Raton, 2nd edition, 2009.

[3] D. H. Hubel and T. N. Wiesel. *Brain and Visual Perception: The Story of a 25-Year Collaboration.* Oxford University Press, Oxford, 2004.

[4] L. da F. Costa. On similarity. https://www.researchgate.net/publication/355792673_On_Similarity, 2021. [Online; accessed 21-Aug-2021].

[5] L. da F. Costa. Multisets. https://www.researchgate.net/publication/355437006_Multisets, 2021. [Online; accessed 21-Aug-2021].

[6] L. da F. Costa. Further generalizations of the Jaccard index. https://www.researchgate.net/publication/355381945_Further_Generalizations_of_the_Jaccard_Index, 2021. [Online; accessed 21-Aug-2021].

[7] J. Hein. *Discrete Mathematics.* Jones & Bartlett Pub., 2003.

[8] D. E. Knuth. *The Art of Computing.* Addison Wesley, 1998.

[9] W. D. Blizard. Multiset theory. *Notre Dame Journal of Formal Logic*, 30:36—66, 1989.

[10] W. D. Blizard. The development of multiset theory. *Modern Logic*, 4:319–352, 1991.

[11] P. M. Mahalakshmi and P. Thangavelu. Properties of multisets. *International Journal of Innovative Technology and Exploring Engineering*, 8:1–4, 2019.

[12] D. Singh, M. Ibrahim, T. Yohana, and J. N. Singh. Complementation in multiset theory. *International Mathematical Forum*, 38:1877–1884, 2011.

[13] L. da F. Costa. Multiset signal processing and electronics. https://www.researchgate.net/publication/355954430_Multiset_Signal_Processing_and_Electronics, 2021. [Online; accessed 21-Nov-2021].

[14] L. da F. Costa. Comparing cross correlation-based similarities. https://www.researchgate.net/publication/355546016_Comparing_Cross_Correlation-Based_Similarities, 2021. [Online; accessed 21-Oct-2021].